Polarization rotation and multiphase coexistence for $Pb(Mg_{1/3}Nb_{2/3})O_3$-$PbTiO_3$ single crystals at the morphotropic phase boundary under electric loading

F. Fang,[1,*] Xu Luo,[1] and W. Yang[2,1]
[1]*AML, School of Aerospace, Tsinghua University, Beijing 100084, China*
[2]*The University Office, Zhejiang University, Hangzhou 310058, China*
(Received 20 January 2009; revised manuscript received 30 March 2009; published 29 May 2009)

In situ observations of the domain evolution and the polarization rotation under bipolar cyclic and static electric fields are carried out for [001]-oriented $68Pb(Mg_{1/3}Nb_{2/3})O_3$-$32PbTiO_3$ (PMN-32PT) single crystal which is located at the morphotropic phase boundary (MPB). The results demonstrate that after being poled in [001] direction, the original rhombohedral (R) phase is transformed into a monoclinic M_C phase with Pm space group. When the single crystal is subjected to bipolar cyclic electric field, distinct domain-boundary structures are revealed which are unlikely to be detected in static electric loadings. The existence of R phase is also detected during the polarization reversal. Under static electric field, polarization rotation from M_C to R occurs and, as the field increases, phase transition from M_C to tetragonal (T) phase takes place. In the vicinity of regions where M_C-T phase transition takes place, polarization reversal of M_C phase is observed, which is attributed to the local stress field from the strain compatibility between the transitioned area and the nontransitioned area. With the removal of the field, T and M_C phases retain while R phase reverses to M_C phase. The results demonstrate that the energy differences among M_C, R, and T phases are rather slim. Accordingly, the multiphase coexistence and polarization rotation under both cyclic and static electric loadings might be responsible for the ultrahigh piezoelectric response of the [001]-oriented rhombohedral $Pb(Mg_{1/3}Nb_{2/3})O_3$-$PbTiO_3$ single crystals near the MPB.

DOI: 10.1103/PhysRevB.79.174118 PACS number(s): 77.80.Dj, 77.22.Ej

I. INTRODUCTION

Single crystals of $(1-x)Pb(Mg_{1/3}Nb_{2/3})O_3$-$xPbTiO_3$ (PMN-xPT) and $(1-x)Pb(Zn_{1/3}Nb_{2/3})O_3$-$xPbTiO_3$ (PZN-xPT) near their morphotropic phase boundaries (MPBs) are under extensive investigations for their extraordinary high dielectric and piezoelectric behaviors.[1–9] Applications of those single crystals caused breakthrough in ultrasonic transducer materials and devices.[10,11] Understanding the relationship between the structure and giant piezoelectric properties is an extremely difficult yet intriguing task. Various mechanisms have been proposed, such as engineered domain configuration, where four variants of crystallographic polarization coexist,[3–5] polarization rotation so that phase transition from rhombohedral (R) to tetragonal (T) phase occurs,[1–3,6,7] random fields, and symmetry-adaptive ferroelectric mesostates.[8,9]

Both theoretical and experimental studies demonstrate that the high piezoelectric behaviors are closely related to the existence of the monoclinic (m) phases, i.e., the m phases act as "structural bridges," allowing or facilitating polarization rotations in the PZN-PT and PMN-PT single crystals.[6,7,12] Based on the first-principles calculation, Fu and Cohen[6] showed that under an electric field applied along [001] direction, polarization rotation could induce a large piezoelectric response for a rhombohedral ferroelectric single crystal. Consequently, phase transition from R to T phase occurs via an intermediate m phase (or phases). They also calculated the free energies along the two possible rotation paths between the R and T phases. By means of an eighth-order expansion of the Landar-Ginzburg-Devonshire free-energy function, instead of a standard sixth order, Vanderbilt and Cohen[13] were able to predict the existence of two different monoclinic phases, with Cm space group (denoted as M_A or M_B) and Pm space group (denoted as M_C), along with the T, R, and orthorhombic (O) phases. Experimentally, the existence of three types of the monoclinic phases, namely, M_A, M_B, and M_C phases in PMN-xPT has been proved by x-ray diffraction,[14–19] neutron diffraction,[20–22] and polarized light microscopy.[23–27] Generally, M_A and M_C are found in a ⟨001⟩-oriented PMN-PT or PZN-PT single crystal near the MPB when poled in ⟨001⟩ directions, while M_B is mostly found for ⟨011⟩-oriented crystals when poled in ⟨011⟩ directions.[19,20,26]

Since the best piezoelectric properties were obtained for ⟨001⟩-oriented PMN-PT and PZN-PT single crystals near the morphotropic phase boundary (MPB), the evolution of their domain structure under external electric loadings should be of particular importance. In unpoled PMN-PT single crystals with a composition close to the MPB, according to the phase diagram proposed by Noheda *et al.*,[15] one or two m phases are expected to occur, along with the T and R phases. By using optical polarized microscope, Xu *et al.*[23] observed the coexistence of M_A and R phases in the as-grown PMN-33PT. Bao *et al.*[27] confirmed the coexistence of M_A and M_C phases in the as-grown PMN-32PT. By using x-ray diffraction techniques, Singh *et al.*[18,22] reported that the MPB for PMN-xPT located at $0.26<x<0.35$, namely, the structure is of T phase for PMN-xPT with $x\geq 0.35$ and is of R phase for PMN-xPT with $x\leq 0.26$. In the MPB regions, M_A is stable for $0.27\leq x\leq 0.30$, while M_C is stable for $0.31\leq x\leq 0.34$.[22] The same progression of R-M_A-M_C-T with increasing PT content was also confirmed by optical microscope investigations.[28] By using neutron Rietveld analysis, Kiat *et al.*[20] reported that the monoclinic phase in PMN-35PT was of M_C phase. The existence of M_C phase was also detected in a ⟨001⟩-oriented

poled PMN-33PT single crystal using polarized light microscope.[25] For ⟨001⟩-oriented poled PMN-35PT single crystal, however, M_A phase was revealed using synchrotron x-ray diffraction.[14] Upon the application of an electric field along the [001] direction, the polarization rotation path of R-M_A-M_C-T was identified by many *in situ* experiments for rhombohedral crystals near MPB.[16,17,29,30]

All these results indicate that the domain structures of PMN-PT around the MPB are versatile and rather intricate, depending sensitively on the composition variation, orientation, and previous loading history. Therefore, more systematic studies are required to better understand the domain structure and polarization rotation under the applied electric fields. Apart from the x-ray and neutron diffraction techniques, optical polarized microscopy observation is an effective way to detect the symmetry of the PMN-PT single crystals. In this paper, *in situ* observations of the domain-structure evolution under both bipolar cyclic and static electric field are carried out for PMN-32PT single crystal which is located at the MPB. The phase is detected by both the optical extinction direction and the permissible domain-boundary structures. The observed domain-structure evolution and phase transition under both cyclic and static electric loadings would be helpful for better understanding of the ultrahigh piezoelectric performances of PMN-PT single crystals at the MPB.

II. EXPERIMENTAL PROCEDURES

The PMN-32PT single-crystal samples were used in this investigation. The composition was determined by measuring their Curie temperature. PMN-PT single crystals were grown directly from the melt by a modified Bridgman technique.[31] The samples were edge oriented parallel to ⟨001⟩ by using an x-ray diffractometer. They were cut and polished into a size of approximately $0.1 \times 5 \times 5$ mm^3. Note that the orientation in this paper is based on the axis of prototype cubic phase of perovskite structure. It is known that single crystals of PMN-PT usually exhibit spatial composition inhomogeneities and the composition in different areas may vary. Based on the lattice symmetry, when the single-crystal sample is observed along the crystallographic ⟨001⟩ direction under cross-polarized light, domains of the T phase exhibit optical extinctions when the polarizer is set along the ⟨100⟩ or ⟨010⟩ crystallographic direction of the crystal sample. For domains of R phase, they exhibit optical extinction when the polarizer is set along the ⟨110⟩ crystallographic directions. However, for the domains of the m phases, the possible extinction angles are not restricted by the symmetry. In order to avoid the complexity caused by the phase coexistence, we selected our single-crystal samples with R phase.

The samples were gold sputtered, leaving a gap of 1500 μm on the surface. Silver leads were attached to the electrodes with air dry silver paste. The detailed experimental setup can be referred to in Ref. 32. Later, a high-voltage power supply consisting of a function generator (TTI-TG1010 by Thurlby Thandar Instruments Ltd., UK) and a voltage amplifier (Trek-610E-K-CE by Trek Inc., USA) were used to apply both alternating (bipolar, sinusoidal with 0.025 Hz frequency) and static electric fields to the single-crystal specimens. The frequency was chosen so that the detailed domain structure evolution can be revealed.

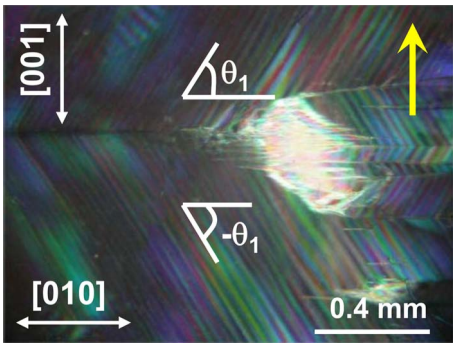

FIG. 1. (Color online) Typical domain configuration for [001]-oriented PMN-32PT single crystal after being poled at 750 V/mm. The arrow in the right-top corner indicates the poling direction.

The single crystals were first poled at a field of 750 V/mm, which was well above the coercive field (approximately 320 V/mm). Then, alternating electric field was applied with the same field magnitude. After several hundreds of electric cycles, the single-crystal sample was again subjected to static electric loading, with the field gradually increasing from 0 to 2500 V/mm. In order to protect against electric breakdown, the specimen was immersed in a silicon oil tank made of transparent and insulating Plexiglas. An Olympus optical microscope with a video imaging system was used to observe and to record changes in the domain configuration. All the micrographs shown in the following paragraphs, unless otherwise specified, were taken under the cross-polarized light and the polarizer forms a 45° angle with the [010] crystallographic direction of the single-crystal sample.

III. RESULTS AND DISCUSSIONS

A. Domain-structure evolution under cyclic electric field

After electric poling at a field magnitude of 750 V/mm, typical morphology of the domain patterns observed under cross-polarized light is shown in Fig. 1. It is seen that the structure is composed of domain twins. Inside each twin, adjacent domains are separated by straight stripes forming an angle of about $\pm\theta_1$ (57.5°) with respect to the [010] crystallographic direction. The twins join together on the (001) crystallographic plane. Since the domains show no extinction, when the polarizer is either set parallel to ⟨011⟩ direction, or to ⟨100⟩ direction, one concludes that the domains belong to monoclinic lattice symmetry.

In PMN-PT single crystals, three types of monoclinic phases, namely, M_A, M_B, and M_C have been reported.[14–27] Since the M_B phase has only been observed in [110]-oriented crystals under the applied electric field, one only needs to consider M_C and M_A phases for a [001]-oriented crystal. For M_C and M_A phases, the polarization vectors lie in the {100} and the {110} crystallographic planes, respectively. There are altogether 24 domain orientations before electric poling for

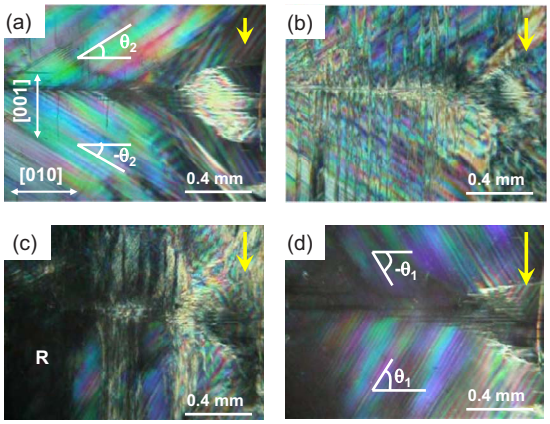

FIG. 2. (Color online) Successive domain-structure changes during the first quarter of the electric cycle at a field magnitude of 750 V/mm. The arrow indicates the electric field direction.

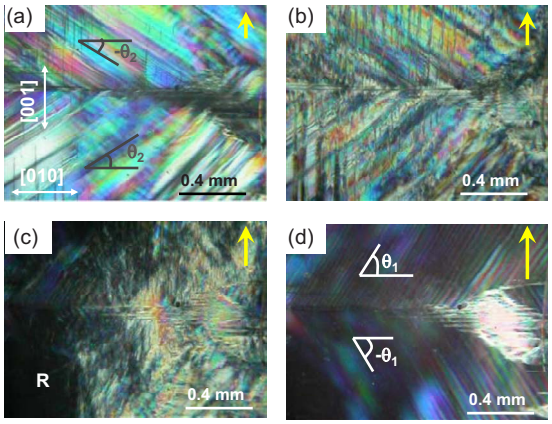

FIG. 3. (Color online) Successive changes in domain structure during the second half of the electric cycle at a field magnitude of 750 V/mm. The arrow indicates the electric field direction.

M_C or M_A phase. After poling, the domains tend to reorient as close as possible to the applied electric field direction, and the possible polarization vectors are reduced to four equivalent directions. The domains with different orientations can be separated by walls of specified orientations that satisfy the conditions of mechanical compatibility and electric neutrality. Bokov and Ye[25] studied the detailed domain-boundary structures for the poled M_A and M_C phases. The agreement between the observed domain-boundary structures with the predictions made there for M_C phase leads to the conclusion that the poled single crystal belongs to the monoclinic M_C phase with Pm space-group symmetry. Our observations that two domain twins join together on (001) plane, or the formation of domain walls in [010] direction, are consistent with their theoretical prediction.[25]

When alternating electric field is applied, the domain patterns show substantial morphology change during the first quarter of a cycle and then exhibits little change during the second quarter. During the last half of the cycle, when the field is reversed, the morphology changes significantly during the third quarter while it keeps unchanged for the fourth quarter. At the end of each cycle, there is almost no apparent morphology change compared with that before electric cycling. This remains true for the single crystal after hundreds of electric cycles.

Figure 2 shows the successive changes in domain pattern during the first quarter of the electric cycle. It can be seen that at the very beginning, straight strips in $\pm\theta_1$ (57.5°) direction gradually rearrange downward and form angles of about $\pm\theta_2$ (32.5°) with respect to [010] direction [Fig. 2(a)]. Then, vertical strips parallel to [001] direction appear and they increase in width and multiply in quantities [Fig. 2(b)]. Later, optical extinction is observed in some areas indicating the appearance of R phase, as designated by "R" in Fig. 2(c). In the lower center of the micrograph in Fig. 2(c), one may find that straight stripes have already reversed their direction, namely, from the originally $-\theta_1$ to θ_1. At the end of the first quarter of the electric cycle, as shown in Fig. 2(d), the domains have changed back to the twin structures with straight strips in each twin, similar to that shown in Fig. 2, but the stripes in each twin are in their opposite directions compared with those before electric cycling (Fig. 1).

During the second half of the electric cycle, when the electric field reverses, almost the same process repeats, as shown in Fig. 3. The parallel stripes that form angles of $\pm\theta_1$ (57.5°) change to $\pm\theta_2$ (32.5°) with respect to [010] direction [Fig. 3(a)], then parallel lines in [001] direction appear [Fig. 3(b)] and later R phase occurs in some area [Fig. 3(c)] and again the domains change back to the original twin structures with the parallel stripes in each twin being reversed [Fig. 3(d)].

Figure 4 depicts the schematics of the polarization reversal process for the M_C phase. Please note that it mainly shows the domain-boundary structures appeared in Figs. 1–3. One may refer to Ref. 25 for all theoretically permissible domain-boundary structures in M_C phase. After poling, the domains align in the four equivalent directions that are closest to the applied poling electric field, as shown in Fig. 4(a). As illustrated in Fig. 4(a) and evidenced in Fig. 1, the adjacent domains denoted as "1" and "2,4" can form domain boundaries along $+\theta_1$ and those denoted as "3" and "2,4" form domain boundaries along $-\theta_1$ directions. The angle of θ_1 (57.5°) depends on the values of the monoclinic lattice parameters.[25]

Upon the reversal of the applied electric field, as shown in Fig. 4(b), the polarization vectors rotate on the {010} planes which they align. They rotate from the equivalent domain variants denoted as "1–4" in Fig. 4(a) to those denoted as "1′–4′," in Fig. 4(b). At the same time, they undergo non-180° domain switching to align themselves on the (002) plane which is perpendicular to the applied electric field direction (denoted as "5–12"). The domain boundaries formed between the adjacent domains denoted as "1′" and "5–8" are just, from the geometric point of view, the boundaries between "3" and "2,4," followed by an anticlockwise rotation of 90° around x axis. The domain boundaries between "3′" and "9–12" are just the boundaries between "1" and "2,4," followed by a clockwise rotation of 90° around x axis. Therefore, θ_2 (32.5°) is just the complementary angle of θ_1 (57.5°), as illustrated in Fig. 4(b) and evidenced in Fig. 2(a).

As illustrated in Fig. 4(c), further increase in the applied electric field causes the polarization switch from "1′–4′" and "5–12" to "1″–4″." During this rotation process, both

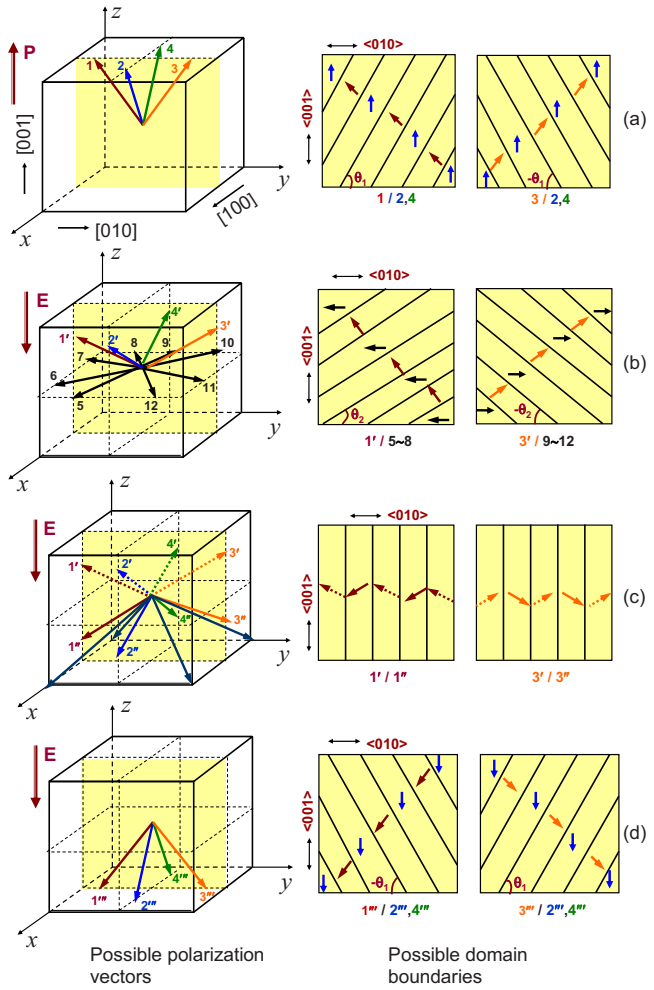

FIG. 4. (Color online) Schematics of polarization reversal for M_C phase. The single-crystal thin plate is based on (100) plane (shadowed) where all the observations are made. The domain boundaries are labeled in accordance with the directions of adjacent domains.

polarization vectors "1′–4′" and "1″–4″" would coexist. Accordingly, adjacent domains of "1" and "1′" or "3" and "3′" would form domain boundaries along the [001] crystallographic direction, as shown in Fig. 2(b).

The appearance of R phase in some area [Fig. 2(c)] indicates the occurrence of polarization rotation from M_C phase ["1″–4″" in Fig. 4(c)] to the four ⟨111⟩ directions aligned with the external electric field, namely, $[1\bar{1}\bar{1}]$, [111], $[11\bar{1}]$, and $[\bar{1}1\bar{1}]$. The occurrence indicates that the energy difference between M_C and R phases is nonsubstantial. At the end of the first quarter of the electric cycle, polarization rotation from R to M_C ("1‴–4‴") takes place, as illustrated in Fig. 4(d). Therefore, straight stripes of angles $\pm\theta_1$ with respect to [010] direction appear. They nevertheless have the reversed direction [Fig. 2(d)] compared to the domain structures shown in Fig. 1. The domain structure evolution during the second half of the electric cycle, as shown in Fig. 3, can also be schematically illustrated by Fig. 4 provided that all the arrows are reversed.

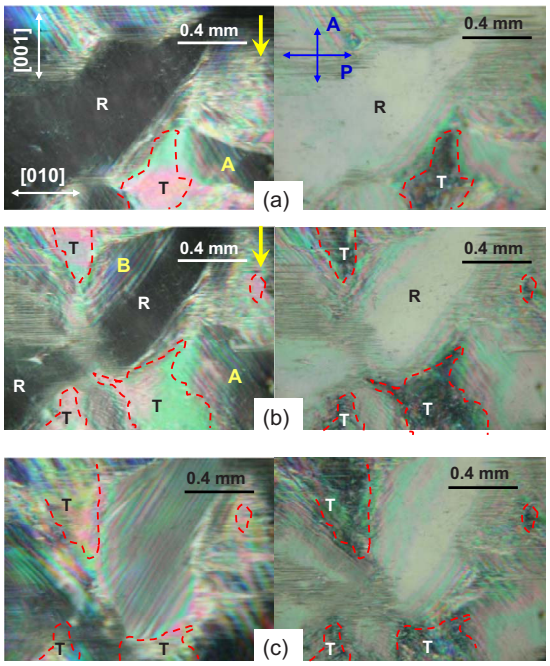

FIG. 5. (Color online) Domain morphology changes when the applied static electric field is (a) 1750, (b) 2200, and (c) 2500 V/mm and followed by complete removal. The micrographs in the right-hand side are taken when the polarizer is set parallel to [010] direction.

B. Polarization rotation under static electric field

Under static electric field, when the field falls below 750 V, the domains of M_C phase undergo their polarization reversal as that shown in Fig. 2 under cyclic electric field. The equivalent domain variants denoted as "1‴–4‴" in Fig. 4(d) would coexist in the single crystal after a static field magnitude of 750 V/mm. With the static electric field further increases, as shown in Fig. 5, substantial morphology changes would take place. First, R phase appears under the electric field which shows optical extinction when the polarizer is set along [011] direction [Figs. 5(a) and 5(b)]. It tends to change back, however, to the parallel stripes in 57.5° direction after the removal of the electric field [Fig. 5(c)]. Second, parallel lines in [010] direction appear. Third, regions exhibiting optical extinctions in [010] direction appear, which are depicted within the red dotted contours of Fig. 5. Fourth, in the vicinity of the regions which show optical extinction along [010] direction, parallel stripes in 57.5° (or −57.5°) with respect to the [010] direction changes their orientation, that is, from the originally 57.5° (or −57.5°) to −57.5° (or 57.5°), such as region "A" in Fig. 5(a) as compared to Fig. 2(d) and region "B" in Fig. 5(b) as compared to Fig. 5(a), It is apparently that region "B" changes its direction partly via R phase.

The occurrence of the R phase upon both the cyclic and static electric fields demonstrates that the energy differences among R and M_C are rather slim, which can be theoretically verified by the Landar-Ginzburg-Devonshire free-energy calculations.[13] Upon the removal of the electric field, the domains tend to adopt the domain-boundary structure of M_C phase, indicating that the formation of domain bands in

$\pm 57.5°$ directions brings the material system to the lowest free-energy state.

For the domain boundaries in [010] direction, the domain bands in that region still belong to M_C phase. This claim is based on the optical extinction direction as well as the theoretically permissible domain-boundary structures postulated by Bokov and Ye.[25] Just as the domain walls in [001] direction can be formed between equivalent domain variants denoted as "1′" and "1″," one may discern from Fig. 4(c) that the domain boundaries in [010] direction can be formed between "1‴" and "3‴" in Fig. 4(d) by an anticlockwise rotation of rotating an angle of 90° around the x axis.

Based on the lattice symmetry, the contoured regions in Fig. 5, where the optical extinction in [010] direction occurs, may belong to either T or M_C phase. The appearance of the reversed domain bands in regions "A" and "B" in Figs. 5(a) and 5(b) will be utilized to identify the "T"-phase nature of these regions. As we know, polarization reversal can be realized by either a reversed electric field or a stress field. Under static electric field, however, no electric-field reversal would occur. Thus, the polarization reversal in the regions "A" and "B" is caused by a strong stress field around them. Domain reversal under stress field was previously reported in $BaTiO_3$ single crystals[33,34] and in PMN-35PT.[35] Without phase transition, the stress field would be insufficient to cause the polarization reversal. On the other hand, sizable strain would be caused if the phase transition from M_C to T phase occurs via polarization rotation. The regions would be elongated along the applied electric-field direction while be contracted along the two other directions normal to it. Due to strain compatibility, the regions where phase transition from M_C-T takes place are constrained by the surrounding nontransitioned matrix. That would induce local tensile stress perpendicular to the applied electric field on adjacent domains such as regions "A" and "B." This local tensile stress drives the domains of M_C phase to reorient by 180°, just as that schematically illustrated in Fig. 4 when the electric field is reversed.

IV. CONCLUSIONS

Phase detections based on the lattice symmetry analysis (optical extinction angle) and the theoretically feasible domain-boundary structures reveal the existence of M_C phase for [001]-oriented PMN-32PT single crystal after poling. When the poled single crystal is subjected to bipolar cyclic electric field, distinctive domain boundaries as well as the occurrence of R phase are revealed. Under static electric field, polarization rotation from M_C to R again occurs and, as the field intensifies, phase transition from M_C to T takes place. In the vicinity of the regions where M_C-T phase transition takes place, polarization reversal of M_C phase is observed, which is attributed to the local stress field from the strain compatibility between the transitioned and the nontransitioned areas. With the removal of the field, T and M_C phases retain while R phase reverses to M_C phase. The coexistence of M_C and R phases under both cyclic and static electric fields demonstrates that their energy difference is rather slim. Accordingly, the multiphase coexistence and polarization rotation under both cyclic and static electric loadings might be responsible for the ultrahigh piezoelectric response of the [001]-oriented rhombohedral $Pb(Mg_{1/3}Nb_{2/3})O_3$-$PbTiO_3$ single crystals near the MPB.

ACKNOWLEDGMENTS

The financial support by the National Natural Science Foundation of China through Grant No. 10772090 and National Basic Research Program of China through Grant No. 2004CB619304 is greatly acknowledged. The authors express sincere thanks to H. S. Luo in Shanghai Institute of Ceramics, Chinese Academy of Sciences, for providing us the single-crystal samples.

*Corresponding author; fangf@mail.tsinghua.edu.cn

[1] J. Kuwata, K. Uchino, and S. Nomura, Ferroelectrics **37**, 579 (1981).
[2] J. Kuwata, K. Uchino, and S. Nomura, Jpn. J. Appl. Phys., Part 1 **21**, 1298 (1982).
[3] S. E. Park and T. R. Shrout, J. Appl. Phys. **82**, 1804 (1997).
[4] S. Liu, S. E. Park, T. R. Shrout, and L. E. Cross, J. Appl. Phys. **85**, 2810 (1999).
[5] S. Wada, S. Suzuki, T. Noma, T. Suzuki, M. Osada, M. Kakihana, S. E. Park, L. E. Cross, and T. R. Shrout, Jpn. J. Appl. Phys., Part 1 **38**, 5505 (1999).
[6] H. Fu and R. E. Cohen, Nature (London) **403**, 281 (2000).
[7] B. Noheda, D. E. Cox, G. Shirane, R. Guo, B. Jones, and L. E. Cross, Phys. Rev. B **63**, 014103 (2000).
[8] D. Viehland, J. Powers, L. E. Cross, and J. F. Li, Appl. Phys. Lett. **78**, 3508 (2001).
[9] D. Viehland, J. Appl. Phys. **88**, 4794 (2000).
[10] S. Saitoh, M. Izumi, S. Shimanuki, S. Hashimoto, and Y. Yamashia, U.S. Patent No. 5,295,487 (22 March 1994).
[11] J. Chen and R. Panda, IEEE International Ultrasounics Symposium Proceedings, Rotterdam, The Netherlands, 2005 (unpublished), Vol. 235.
[12] M. Davis, J. Electroceram. **19**, 23 (2007).
[13] D. Vanderbilt and M. H. Cohen, Phys. Rev. B **63**, 094108 (2001).
[14] Z. G. Ye, B. Noheda, M. Dong, D. Cox, and G. Shirane, Phys. Rev. B **64**, 184114 (2001).
[15] B. Noheda, D. E. Cox, G. Shirane, J. Gao, and Z. G. Ye, Phys. Rev. B **66**, 054104 (2002).
[16] B. Noheda, D. E. Cox, G. Shirane, S. E. Park, L. E. Cross, and Z. Zhong, Phys. Rev. Lett. **86**, 3891 (2001).
[17] B. Noheda, Z. Zhong, D. E. Cox, G. Shirane, S. E. Park, and P. Rehrig, Phys. Rev. B **65**, 224101 (2002).
[18] A. K. Singh and D. Pandey, J. Phys.: Condens. Matter **13**, L931 (2001).
[19] H. Cao, F. M. Bai, N. G. Wang, J. F. Li, D. Viehland, G. Y. Xu,

and G. Shirane, Phys. Rev. B **72**, 064104 (2005).
[20] J. M. Kiat, Y. Uesu, B. Dkhil, M. Matsuda, C. Malibert, and G. Calvarin, Phys. Rev. B **65**, 064106 (2002).
[21] A. K. Singh, D. Pandey, and O. Zaharko, Phys. Rev. B **68**, 172103 (2003).
[22] A. K. Singh and D. Pandey, Phys. Rev. B **67**, 064102 (2003).
[23] G. Xu, H. Luo, H. Xu, and Z. Yin, Phys. Rev. B **64**, 020102(R) (2001).
[24] C. S. Tu, I. C. Shih, V. H. Schmidt, and R. Chien, Appl. Phys. Lett. **83**, 1833 (2003).
[25] A. A. Bokov and Z. G. Ye, J. Appl. Phys. **95**, 6347 (2004).
[26] D. Viehland and J. F. Li, J. Appl. Phys. **92**, 7690 (2002).
[27] P. Bao, F. Yan, X. Lu, J. Zhu, H. Shen, Y. Wang, and H. S. Luo, Appl. Phys. Lett. **88**, 092905 (2006).
[28] D. Zekria, V. A. Shuvaeva, and A. M. Glazer, J. Phys.: Condens. Matter **17**, 1593 (2005).
[29] M. Davis, D. Damjanovic, and N. Setter, Phys. Rev. B **73**, 014115 (2006).
[30] F. Bai, N. Wang, J. Li, D. Viehland, and P. M. Gehring, J. Appl. Phys. **96**, 1620 (2004).
[31] G. S. Xu, H. S. Luo, Y. P. Guo, Y. Q. Gao, H. Q. Xu, Z. Y. Qi, W. Z. Zhong, and Z. W. Yin, Solid State Commun. **120**, 321 (2001).
[32] F. Fang, W. Yang, F. C. Zhang, and H. Qing, J. Mater. Res. **23**, 3387 (2008).
[33] F. Fang and W. Yang, Mater. Lett. **57**, 198 (2002).
[34] D. Fang, Y. Jiang, S. Li, and C. T. Sun, Acta Mater. **55**, 5758 (2007).
[35] J. K. Shang and X. Tan, Acta Mater. **49**, 2993 (2001).